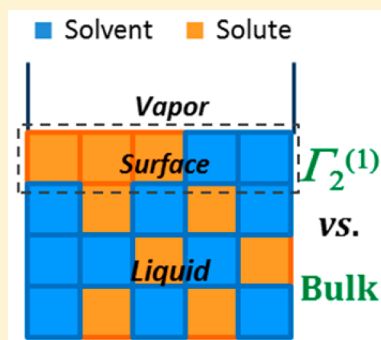


# Gibbs Excess and the Calculation of the Absolute Surface Composition of Liquid Binary Mixtures

Carolina Bermúdez-Salguero and Jesús Gracia-Fadrique\*

Departamento de Fisicoquímica, Facultad de Química, Universidad Nacional Autónoma de México, Ciudad Universitaria, México D.F. 04510, Mexico

**ABSTRACT:** Adsorption at the liquid–vapor interphase of a liquid binary mixture is traditionally quantified by means of the Gibbs solute excess. Despite several theoretical reviews on the meaning of Gibbs excess defined by the Gibbs dividing surface, it is still misinterpreted as the excess concentration under Guggenheim’s finite-depth surface layer approach. In this work, both concepts are clarified in a practical way, aided by a graphical representation without loss of generality. The understanding of both quantities led to the development of a thermodynamic procedure for the calculation of the actual number of solute and solvent molecules at a finite-depth surface layer (not a monolayer), what is called the absolute surface composition. From surface tension and density data, the absolute surface composition of the binary aqueous mixtures of methanol, ethanol, 1-propanol, and 1-butanol was calculated. Results show thermodynamic consistency and agree with experimental reports and with an empirical mixing rule. The increasing alcohol surface concentration throughout the entire concentration range casts doubt on the formation of an alcohol monolayer, as was suggested by other authors. Furthermore, the use of Guggenheim’s monolayer model does not reproduce the experimental data, nor does it show thermodynamic consistency.



## 1. INTRODUCTION

The absolute or total surface composition is claimed to be one of the most difficult properties to assess experimentally and theoretically, yet the properties of any system depend on its composition. Solute adsorption at the liquid–vapor interface of a binary system is traditionally determined from surface tension data by means of the Gibbs adsorption equation.<sup>1–5</sup> However, the Gibbs adsorption equation provides the surface excess of the solute and not the actual number of molecules at a surface layer, what here is called the absolute surface composition. Gibbs excess is a relative quantity that has been thoroughly analyzed from a theoretical perspective in terms of the zero-volume Gibbs dividing surface, as in the latest review of Radke<sup>6</sup> and several other bedside references,<sup>7–10</sup> but there are few attempts to understand its physical meaning in a simple way.<sup>11</sup> In this paper, a graphical representation of Gibbs solute excess is depicted in the most comprehensible form possible, and it is compared with the surface excess defined under Guggenheim’s finite-depth surface layer treatment,<sup>12</sup> which can be easily misinterpreted as the same quantity. From these concepts, quantitative equations were developed for calculating the absolute surface composition of *both* solute *and* solvent in a binary liquid mixture, and not only of solute as is the common practice.<sup>3–5</sup> Surface tension and density are the primary data needed. Surface molar fractions were derived easily from the absolute surface concentrations.

Different models correlate surface tension with surface composition; lists of these models have been given elsewhere.<sup>13,14</sup> Among them, the simplicity of the mixing rules of Eberhart<sup>15</sup> (eq 1) and Laaksonen<sup>16</sup> (eq 2) has contributed to their use in the derivation of more complex phenomenological

models.<sup>13,17</sup> However, there are few works committed to verify its validity, like those of Salonen et al.<sup>14</sup> and Raina et al.<sup>18,19</sup>

$$\sigma = x_1^s \sigma_1 + x_2^s \sigma_2 \quad (1)$$

$$\sigma = \phi_1^s \sigma_1 + \phi_2^s \sigma_2 \quad (2)$$

In eqs 1 and 2,  $\sigma$  is the surface tension of the mixture,  $\sigma_1$  and  $\sigma_2$  are the surface tensions of the pure compounds, and  $x_i^s$  and  $\phi_i^s$  are the molar fraction and the volume fraction of component  $i$  at the surface, respectively. The volume fraction is given by eq 3, where  $\bar{v}_i$  is the partial molar volume of component  $i$ .

$$\phi_i^s = \frac{x_i^s \bar{v}_i}{x_1^s \bar{v}_1 + x_2^s \bar{v}_2} \quad (3)$$

Raina et al. measured the composition of the vapor in direct contact with the surface of aqueous binary mixtures of methanol, ethanol, 1-propanol, and 1-butanol. The vapor was swept off the surface through a pulsed supersonic valve, and surface molar fractions were determined by means of TOF–mass spectrometry. Salonen et al. compared Raina et al.’s results with the Eberhart and Laaksonen rules and with their own density functional theory (DFT) calculations, agreeing with Raina et al. that the Laaksonen rule predicts correctly the surface composition of the binary aqueous systems of the  $n$ -alcohols. The Eberhart rule was discarded.

**Received:** February 11, 2015

**Revised:** April 7, 2015

**Published:** April 8, 2015

The procedure developed in this work for the calculation of the absolute surface composition was applied to the aqueous binary mixtures of the same alcohols studied by Raina et al. at 298.15 K, with surface tension and density data taken from the literature. Surface molar fractions very close to Raina et al.'s data and the Laaksonen rule were obtained. However, for ethanol and 1-propanol, a decreasing behavior of surface molar fractions with increasing bulk concentration was detected within a certain interval. Results show that this unlikely behavior is due to experimental errors in the surface tension and not due to the procedure itself, where the starting point is the determination of the Gibbs solute excess. Gibbs solute excess can also be obtained, for instance, from neutron reflection experiments as done by Li et al.,<sup>20–22</sup> if Li et al.'s data are used, anomalies disappear and the surface composition shows a constant increasing behavior over the entire composition range. Raina et al. also compared their results with Li et al.'s,<sup>20</sup> but confusion on surface excess quantities shadowed their achievements; actually, their results are more accurate than they thought.

The only nonthermodynamic approach for the calculation of absolute surface composition is the estimation of the surface thickness from the partial molar volume of the alcohols. The impact of the thickness on surface composition is analyzed. However, the surface composition predicted in this paper is proved to be thermodynamically consistent with the Gibbs–Duhem equations from which the procedure was developed because the influence of surface thickness is canceled in the consistency test, leaving under scrutiny the thermodynamic equations alone.

In the extensively cited work of Yano,<sup>23</sup> it has been claimed that methanol, ethanol, 1-propanol, 2-propanol, and *tert*-butanol form a monolayer over their aqueous binary solutions. The explanation of Yano relies on the fact that the Gibbs excess of the alcohols attains a maximum at a given bulk concentration and that its reciprocal agrees approximately with an area of 20 Å<sup>2</sup> per CH<sub>2</sub> chain in a close-packed configuration. According to the physical meaning of Gibbs excess, a maximum is expected, but it does not imply that the absolute surface concentration attains a maximum too, as will be shown in this work. Furthermore, Gibbs excess shall not be interpreted as the absolute surface concentration so as to obtain an area per molecule. Salonen et al.<sup>14</sup> have calculated the surface molar fractions of alcohols following Guggenheim's monolayer approach, pointing out its failure to predict the experimental data, obtaining surface molar fractions >1. We decided to include our own calculations with the monolayer model to show that if consistent areas are used, no molar fractions >1 are obtained. Despite this effort, surface composition obeying a monolayer model does not reproduce the experimental data of Raina et al., and it does not show thermodynamic consistency with the Gibbs–Duhem equations. Together with the constant increasing behavior of the alcohols' surface concentration, the formation of a monolayer of soluble alcohols is doubtful.

## 2. THEORY

### 2.1. Gibbs Excess, Surface Excess, and Absolute Two-Dimensional Surface Concentration in Binary Mixtures.

If the surface of a liquid binary mixture at the liquid–vapor interface is regarded as an additional thermodynamic phase, the chemical potentials of the solvent and the solute,  $\mu_1$  and  $\mu_2$ , respectively, are related through the Gibbs–Duhem equation of the surface<sup>7</sup> (eq 4)

$$N_1^s d\mu_1 + N_2^s d\mu_2 = -\mathcal{A} d\sigma \quad \text{constant } T, p \quad (4)$$

where  $\sigma$  is the surface tension of the mixture,  $\mathcal{A}$  is the area of the surface, and  $N_1^s$  and  $N_2^s$  are the number of moles of solvent and solute at the surface, respectively. If the surface is in equilibrium with the liquid, chemical potentials are also related by the Gibbs–Duhem equation of the liquid phase<sup>6,24</sup> (eq 5)

$$N_1 d\mu_1 + N_2 d\mu_2 = 0 \quad \text{constant } T, p \quad (5)$$

where  $N_1$  and  $N_2$  are the number of moles in the liquid phase. Substitution of eq 5 into eq 4 for the elimination of  $d\mu_1$  leads to the Gibbs adsorption equation (eq 6)

$$\Gamma_2^{(1)} d\mu_2 = -d\sigma \quad (6)$$

where the Gibbs surface excess of the solute  $\Gamma_2^{(1)}$  is defined by eq 7, in terms of the absolute two-dimensional surface concentrations,  $\Gamma_1$ , and  $\Gamma_2$ .

$$\Gamma_2^{(1)} \equiv \Gamma_2 - \Gamma_1 \frac{N_2}{N_1} \quad (7)$$

The absolute two-dimensional surface concentrations are the number of moles of each component per unit area, defined by eq 8.

$$\Gamma_i = \frac{N_i^s}{A} \quad (8)$$

The understanding of the physical meaning of  $\Gamma_2^{(1)}$  is fundamental for the calculation of  $\Gamma_1$  and  $\Gamma_2$ , as will be explained qualitatively in the following paragraphs. Quantitative calculations from experimental surface tension and density data are presented in section 2.2.

Consider the binary system in Figure 1a. The system represents a liquid phase with a liquid–vapor (LV) interface of

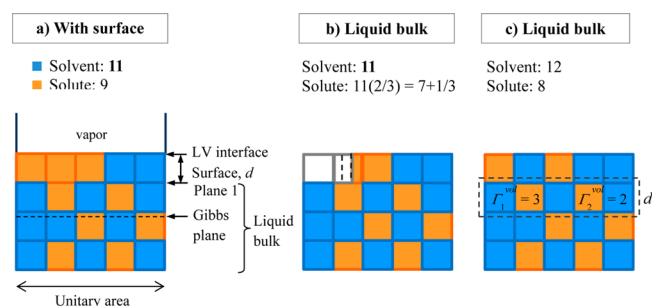


**Figure 1.** (a) Liquid binary system with a LV interface; (b) liquid bulk phase with the same amount of solvent as in (a); (c) liquid bulk system with the same volume as in (a).

unitary area. Molecules are represented by squares for the sake of clarity; blue squares are solvent molecules, and orange squares are solute molecules. In the liquid bulk, the solute/solvent molar proportion is  $N_2/N_1 = 2/3$ . At the LV interface, where the solute adsorbs defining a finite-depth surface (between the LV interface and plane 1), the absolute two-dimensional concentration of solute is  $\Gamma_2 = 3$  and the concentration of solvent is  $\Gamma_1 = 2$ . According to eq 7, the Gibbs surface excess of the solute  $\Gamma_2^{(1)}$ , hereafter the Gibbs excess, is the difference between the actual solute surface concentration  $\Gamma_2$  and the solute concentration that would exist if the surface composition were equal to the bulk ratio  $N_2/N_1$ ,

that is, if the solute surface concentration were  $\Gamma_1(N_1/N_2)$ . In the example, Gibbs excess is  $\Gamma_2^{(1)} = 3 - 2(2/3) = 1 + 2/3$ .

In the system of Figure 1a, there are a total of 11 solvent molecules and 9 solute molecules. In the system of Figure 1b, which represents a liquid bulk system with the same bulk composition as the former, there are also 11 solvent molecules, but  $11(2/3) = 7 + 1/3$  solute molecules. The difference between the amount of solute in both systems provides the Gibbs excess,  $\Gamma_2^{(1)} = 9 - (7 + 1/3) = 1 + 2/3$ . Therefore,  $\Gamma_2^{(1)}$  is the difference between the amount of solute in two systems, one system with a surface and the other without it, both with the same amount of solvent.<sup>12</sup> Note that although in Figure 1a the surface is a monolayer, the analysis presented is not restricted to such a model.

Gibbs excess defines the Gibbs dividing surface, or Gibbs plane, located at a distance from the LV interface such that the amount of solvent in the surface (between the LV interface and Gibbs plane in Figure 1a) is the same as in the bulk solution.<sup>8,12</sup> In the example, the Gibbs plane is located  $(2^{1/6})$ th beneath the LV interface, obtaining 5.5 solvent molecules at both sides of the Gibbs plane. The difference between the amount of solute in both sides (equivalent to compare a system with a surface with another without it) provides  $\Gamma_2^{(1)} = (5 + 1/3) - (2 + 5/3) = 1 + 2/3$ , showing that the Gibbs excess does not depend on the size of the system (with 11 or 5.5 water molecules) or on the location of the plane that divides the surface from the bulk (plane 1 or Gibbs plane);<sup>11</sup> with Gibbs plane, obeying eq 7,  $\Gamma_2^{(1)} = (5 + 1/3) - 5.5(2/3) = 1 + 2/3$ .

Gibbs excess can be obtained from the Gibbs adsorption equation from the substitution of the solute chemical potential given by eq 9 into eq 6, providing eq 10, known also as Gibbs adsorption equation.<sup>10</sup>

$$\mu_2 = \mu_2^0 + RT \ln a_2 \quad (9)$$

$$\Gamma_2^{(1)} = \frac{1}{RT} \left( \frac{d\pi}{d \ln a_2} \right) \quad (10)$$

The activity of the solute  $a_2$  is the product of the bulk molar fraction  $x_2$  and the activity coefficient  $\gamma_2(x_2)$ ,  $a_2 = x_2\gamma_2(x_2)$ .<sup>25</sup> The surface tension  $\sigma$  in eq 6 has been replaced in eq 10 by the surface pressure  $\pi$ , defined as the difference between the surface tension of the pure solvent and the surface tension of the mixture,  $\pi = \sigma_1 - \sigma$ . According to eq 10, Gibbs excess can be calculated from the slope of the curve  $\pi$  versus  $\ln a_2$ , indicating that  $\Gamma_2^{(1)}$  does not depend on the plane delimiting the surface from the bulk or on the size of the system, because  $\pi$  and  $a_2$  are intensive experimental variables. If surface pressure is an increasing function of solute concentration,  $\Gamma_2^{(1)}$  is a positive quantity, indicating solute adsorption.

From surface tension data, Gibbs excess can be computed to determine the total number of solute molecules contained in a system with a given amount of solvent. In the example of Figure 1a, for a system with 11 solvent molecules, there are  $11(2/3) + (1 + 2/3) = 9$  molecules of solute. From this information, however, it is not possible to obtain the absolute surface concentrations  $\Gamma_1$  and  $\Gamma_2$  because the distribution of the components between the bulk and the surface remains unknown; that is, in practice, Figure 1a is not available.

The comparison of two systems with the same volume, one system with a LV interface (Figure 1a) and the other without it (Figure 1c), provides the deficit of solvent and the excess of solute in the system with the LV interface, due to solute

adsorption.<sup>12</sup> The differences between the amount of solute and solvent in these two systems were named *two-dimensional surface excess concentrations*, hereafter *excess concentrations*,  $\Gamma_1^{\text{exc}}$  and  $\Gamma_2^{\text{exc}}$ . In the system of Figure 1c, with the same volume of the system in Figure 1a, there are 12 solvent molecules and 8 solute molecules, keeping the proportion  $N_2/N_1 = 2/3$  of Figure 1a. Hence, the solvent deficit is  $\Gamma_1^{\text{exc}} = 11 - 12 = -1$ , and the solute excess is  $\Gamma_2^{\text{exc}} = 9 - 8 = 1$ . For a pure compound, the excess concentration is null.

Let us define the *two-dimensional volumetric concentrations*,  $\Gamma_1^{\text{vol}}$  and  $\Gamma_2^{\text{vol}}$ , as the amount of solvent and solute in an area occupied by a volume with the same thickness  $d$  of the surface, as illustrated in Figure 1c, with  $\Gamma_1^{\text{vol}} = 3$  and  $\Gamma_2^{\text{vol}} = 2$ . If the two-dimensional volumetric concentrations  $\Gamma_i^{\text{vol}}$  are added to the excess concentrations  $\Gamma_i^{\text{exc}}$ , the result is the absolute concentrations,  $\Gamma_i = \Gamma_i^{\text{exc}} + \Gamma_i^{\text{vol}}$ , being  $\Gamma_1 = -1 + 3$  and  $\Gamma_2 = 1 + 2 = 3$ , as in Figure 1a. Quantitative calculation of  $\Gamma_i$  from  $\Gamma_i^{\text{vol}}$ ,  $\Gamma_i^{\text{exc}}$ , and  $\Gamma_2^{(1)}$  is presented in section 2.2.

**2.2. Absolute Two-Dimensional Surface Concentrations from Surface Tension and Density Data.** A binary mixture with a LV interface of unitary area contains  $N_2$  moles of solute per  $N_1$  moles of solvent plus  $\Gamma_2^{(1)}$  moles of solute. The proportion  $N_2/N_1$  is equal to the quotient of bulk molar fractions  $x_2/x_1$ . Taking a calculation base of 1 mol of solvent and  $(x_2/x_1 + \Gamma_2^{(1)})$  moles of solute, the volume  $V$  of the system is given by eq 11

$$V = \bar{v}_1 + \left( \frac{x_2}{x_1} + \Gamma_2^{(1)} \right) \bar{v}_2 \quad (11)$$

where the partial molar volumes  $\bar{v}_1$  and  $\bar{v}_2$  are considered equal in the bulk and in the surface. Partial molar volumes can be determined from the molar volume  $v$  of the mixtures through eqs 12 and 13:<sup>26</sup>

$$\bar{v}_1 = v - x_2 \left( \frac{\partial v}{\partial x_2} \right)_{T,p} \quad (12)$$

$$\bar{v}_2 = v + x_1 \left( \frac{\partial v}{\partial x_2} \right)_{T,p} \quad (13)$$

The molar volume  $v$  is given by eq 14

$$v = \frac{x_1 M_1 + x_2 M_2}{\rho} \quad (14)$$

where  $M_1$  and  $M_2$  are the molar masses of each component and  $\rho$  is the mass density of the mixture.

The volume  $V$  of a liquid bulk system, without interface, is given by eq 15:

$$V = N_1 \bar{v}_1 + N_2 \bar{v}_2 \quad (15)$$

Dividing eq 15 by  $N_2$  to obtain the quotient  $x_1/x_2$  provides eq 16, which allows the calculation of the amount of solute  $N_2^b$  contained in a liquid bulk phase with the same volume  $V$  of the system with the LV interface.

$$N_2^b = \frac{V}{\left( \frac{x_1}{x_2} \bar{v}_1 + \bar{v}_2 \right)} \quad (16)$$

The number of moles  $N_2$  in eq 16 has been distinguished with the superscript "b" to emphasize that it is the amount of solute

within a *bulk* phase. The amount of solvent is obtained from the proportion  $x_1/x_2$  by means of eq 17.

$$N_1^b = \left( \frac{x_1}{x_2} \right) N_2^b \quad (17)$$

The difference between the amount of solute in the system with a LV interface ( $x_2/x_1 + \Gamma_2^{(1)}$ ) and the amount of solute in the bulk phase  $N_2^b$  yields the excess concentration  $\Gamma_2^{\text{exc}}$  (eq 18).

$$\Gamma_2^{\text{exc}} = \left( \frac{x_2}{x_1} + \Gamma_2^{(1)} \right) - N_2^b \quad (18)$$

The solvent excess concentration is given by eq 19.

$$\Gamma_1^{\text{exc}} = 1 - N_1^b \quad (19)$$

Excess concentrations may be either positive or negative quantities depending on the surface activity of each component. If the solute is adsorbed,  $\Gamma_2^{\text{exc}}$  is positive, whereas the solvent excess  $\Gamma_1^{\text{exc}}$  is negative, as in the comparison of the systems in panels a and c of Figure 1.

The two-dimensional volumetric concentrations,  $\Gamma_i^{\text{vol}}$  and  $\Gamma_2^{\text{vol}}$ , can be computed from the bulk molar concentration of each component ( $x_i/v$ ), multiplied by the thickness  $d$  of the surface (eq 20). Estimation of the thickness will be discussed in section 2.3.

$$\Gamma_i^{\text{vol}} = \frac{x_i}{v} d \quad (20)$$

The absolute two-dimensional concentrations,  $\Gamma_1$  and  $\Gamma_2$ , are obtained from the addition of the excess and the two-dimensional volumetric concentrations (eq 21)

$$\Gamma_i = \Gamma_i^{\text{exc}} + \Gamma_i^{\text{vol}} \quad (21)$$

for finally achieving the surface molar fractions  $x_i^s$  through eq 22:

$$x_i^s = \frac{\Gamma_i}{\Gamma_1 + \Gamma_2} \quad (22)$$

Equations 11–22 will be applied in section 3.1 to the aqueous binary mixtures of methanol, ethanol, 1-propanol, and 1-butanol to determine the absolute surface composition.

**2.3. Estimation of the Surface Thickness.** The surface of a binary mixture of miscible or partially miscible components is constituted by both solvent and solute molecules. The finite-depth surface model adopted in this work is illustrated in Figure 2, where the thickness  $d$  of the surface layer next to the LV interface is defined by the component with the largest volume. Note that it is not a monolayer model.

If molecules are considered as spheres of diameter  $d$ , the surface thickness is afforded through eq 23

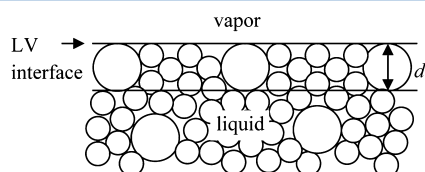


Figure 2. Finite-depth surface model.

$$d = \left( \frac{6}{\pi} \frac{\bar{v}_2}{N_{\text{Av}}} \right)^{1/3} \quad \text{for } \bar{v}_2 > \bar{v}_1 \quad (23)$$

where  $N_{\text{Av}}$  is Avogadro's number. This approach has also been used by other authors;<sup>18,19</sup> Douillard points out that from different experimental techniques and molecular computer simulations, the surface has been estimated to be 1–1.5 molecular diameters thick.<sup>27</sup> The impact of the thickness on the surface composition will be analyzed in section 3.3.

**2.4. Guggenheim's Monolayer Approach.** An alternative to calculate the absolute surface composition is adopting Guggenheim's monolayer approach,<sup>12</sup> in which the area  $\mathcal{A}$  of the surface is given by the addition of the partial molar areas of each component,  $\bar{a}_1$  and  $\bar{a}_2$ , obeying eq 24.

$$\mathcal{A} = N_1^s \bar{a}_1 + N_2^s \bar{a}_2 \quad (24)$$

If eq 24 is divided by  $\mathcal{A}$ , a relationship between  $\Gamma_1$  and  $\Gamma_2$  is obtained (eq 25),

$$\bar{a}_1 \Gamma_1 + \bar{a}_2 \Gamma_2 = 1 \quad (25)$$

From eq 25, the solvent concentration  $\Gamma_1$  can be determined from the solute concentration  $\Gamma_2$ .

An inconvenience of this approach is the availability of the partial molar areas. A common practice is to assume the squared projection of a sphere of volume  $\bar{v}_i$ , as proposed by Sprow and Prausnitz<sup>28–30</sup> (eq 26).

$$\bar{a}_i = N_{\text{Av}}^{1/3} \bar{v}_i^{2/3} \quad (26)$$

To reduce the influence of the assumption of spherical geometry, molecules can be considered as rectangular prisms of volume  $\bar{v}_i$  and height  $d$ , projecting an area on the surface given by eq 27.

$$\bar{a}_i = \frac{\bar{v}_i}{d} \quad (27)$$

For the Guggenheim monolayer approach, the maximum feasible partial molar area of the solute is the reciprocal of the two-dimensional concentration  $\Gamma_2$ . Otherwise, eq 25 would yield negative solvent concentrations and, thus, solute surface molar fractions  $>1$  (eq 22). The maximum two-dimensional concentration of the solute is  $\Gamma_2^{\text{pure}}$  equal to its two-dimensional volumetric concentration  $\Gamma_2^{\text{vol}}$  (see eq 21 with  $\Gamma_i^{\text{exc}} = 0$ ). Thus, according to eq 20 with  $x_i = 1$ , the minimum feasible area is given by eq 28

$$\bar{a}_i^{\text{min}} = \frac{1}{\Gamma_i^{\text{pure}}} = \frac{v_i}{d} \quad (28)$$

where  $v_i$  is the molar volume of the pure compound. Evaluation of eq 27 for a pure compound leads to eq 28. Thus, partial molar areas will be calculated using eq 27. Besides, Sprow and Prausnitz approximation provides areas larger than the reciprocal of  $\Gamma_2$ .

**2.5. Thermodynamic Consistency of the Surface Composition.** The thermodynamic consistency of the procedure developed in section 2.2 for the calculation of the absolute surface composition of a binary mixture can be verified by means of the same thermodynamic equations from which it was developed.

If the Gibbs–Duhem equations of the surface and the bulk are combined (eqs 4 and 5), the Gibbs adsorption equation is obtained (eq 6). If eq 6 is substituted back into eq 4, an



expression for the chemical potential of the solvent arises (eq 29).

$$d\mu_1 = \left[ \frac{1}{\Gamma_1} - \frac{x_2^s}{x_1^s} \frac{1}{\Gamma_2^{(1)}} \right] d\pi \quad (29)$$

Integration of eq 29, from  $\pi = 0$  to  $\pi$ , affords the difference between the chemical potential of the solvent in the mixture and the chemical potential of the pure solvent  $\mu_1^0$  (eq 30).

$$\mu_1 - \mu_1^0 = \int_0^\pi \left[ \frac{1}{\Gamma_1} - \frac{x_2^s}{x_1^s} \frac{1}{\Gamma_2^{(1)}} \right] d\pi \quad (30)$$

Equation 30 should provide the same result as eq 31

$$\mu_1 - \mu_1^0 = RT \ln a_1 \quad (31)$$

where the activity of the solvent  $a_1$  is the product of the bulk molar fraction  $x_1$  and the activity coefficient  $\gamma_1(x_1)$ ,  $a_1 = x_1\gamma_1(x_1)$ .<sup>25</sup>

### 3. RESULTS AND DISCUSSION

**3.1. Surface Composition Determined from Surface Tension and Density Data.** The surface compositions of the binary aqueous mixtures of methanol, ethanol, 1-propanol, and 1-butanol were determined from surface tension data by applying the procedure described in section 2.2. Surface tension was taken from the literature. The sources were selected on the basis of the number of experimental data points and the accurate prediction of the alcohols' activity coefficients at infinite dilution in water  $\gamma_2^\infty$  from surface tension data.<sup>3</sup> For the methanol system, Vázquez et al.'s data<sup>31</sup> at 298.15 K does not provide the right activity coefficient as Livingston et al.'s data<sup>32</sup> at 303.15 K. For the systems of ethanol and 1-propanol, surface tension was taken from Strey et al.'s paper<sup>5</sup> at 298.15 K; in both systems, surface tension agrees with the values reported by Vázquez et al., but the number of experimental points is higher in Strey et al.'s work. For the partially miscible aqueous system of 1-butanol, Habrdoová et al.<sup>33</sup> reported surface tensions up to a molar fraction of 1-butanol  $x_2 = 0.0141$  at 298.15 K.

The activity of the alcohols,  $a_2 = x_2\gamma_2$ , was calculated using the activity coefficients  $\gamma_2$  provided by the van Laar model (eq 32)

$$\ln \gamma_2 = B \left( \frac{Ax_1}{Ax_1 + Bx_2} \right)^2 \quad (32)$$

where  $A = \ln \gamma_1^\infty$  and  $B = \ln \gamma_2^\infty$ . The coefficients obey the symmetric convention:  $x_i \rightarrow 1, \gamma_i \rightarrow 1; x_i \rightarrow 0, \gamma_i \rightarrow \gamma_i^\infty$ . Strey et al. showed this model to best fit their own experimental activity data for ethanol and 1-propanol.<sup>5</sup> Yano also chose the van Laar model as the best fit to experimental activities of methanol.<sup>23</sup> The activity coefficients at infinite dilution used in eq 32 are listed in Table 1.

The alcohol's Gibbs excess  $\Gamma_2^{(1)}$  was determined numerically from the slope of the curves  $\pi$  versus  $\ln a_2$ , according to eq 10. Polynomials were fitted to the experimental data as shown in Figure 3, affording correlation coefficients  $R > 0.9990$ . For methanol, a fourth-degree polynomial was chosen. For ethanol, data were divided into two regions because of the difficulty of finding a single polynomial for the whole concentration range; the dilute region ( $0 < x_2 \leq 0.0200$ ) was described by a second-degree polynomial and the concentrated region ( $0.0200 \leq x_2 \leq 1$ ) by a fifth-degree polynomial. Note that the molar fraction  $x_2$

**Table 1. Activity Coefficients at Infinite Dilution of Water in Alcohol  $\gamma_1^\infty$  and of Alcohol in Water  $\gamma_2^\infty$  at 298.15 K**

water (1) + alcohol (2)	$\gamma_1^\infty$	$\gamma_2^\infty$
methanol	1.54 <sup>a</sup>	1.72 <sup>a</sup>
ethanol	2.630 <sup>b</sup>	4.786 <sup>b</sup>
1-propanol	3.631 <sup>b</sup>	13.80 <sup>b</sup>
1-butanol	50.2 <sup>c</sup>	5.41 <sup>c,d</sup>

<sup>a</sup>Reference 34. <sup>b</sup>Reference 5. <sup>c</sup>Reference 35. <sup>d</sup> $T = 308.15$  K.

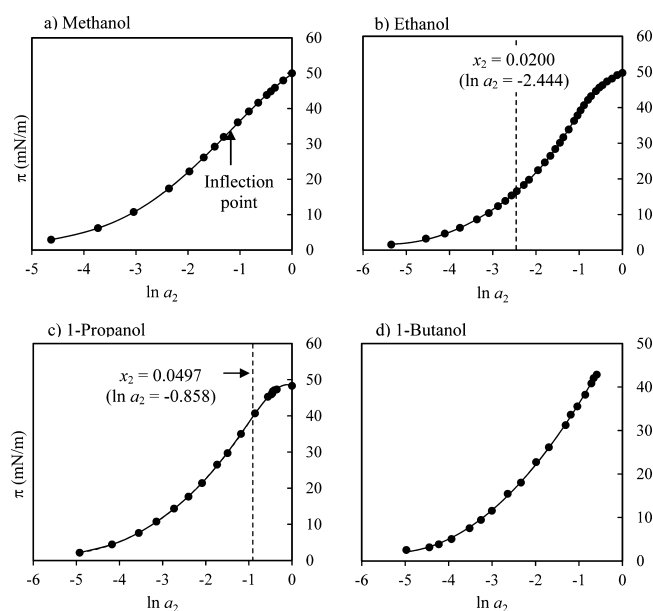


**Figure 3.** Nonlinear fitting of  $n$ th-degree polynomials to the experimental surface pressure  $\pi$  versus the logarithm of the alcohol's activity  $a_2$  at 298.15 K, except for methanol, at 303.15 K.

$= 0.0200$  was included in both fittings, attempting continuity in the adjustments. 1-Propanol data were described by a sixth-degree polynomial in the entire interval. After  $x_2 = 0.0497$ , the fitting might be doubtful, but the same results are obtained with a third-degree polynomial fitted in the interval  $0.0200 \leq x_2 \leq 1$  ( $x_2 = 0.0200$  is two points below  $x_2 = 0.0497$  in Figure 3c). For 1-butanol, a second-degree polynomial provided a satisfactory correlation.

The partial molar volumes  $\bar{v}_1$  and  $\bar{v}_2$  needed for computing the volume  $V$  of a system with a LV interface (eq 11) were determined from density data. Densities of the aqueous systems of methanol and ethanol were reported by González et al.<sup>36</sup> and Zarei et al.<sup>37</sup> at 303.15 K; the two sources agree with each other. For 1-propanol at 298.15 K, densities were interpolated from Zarei et al.'s data<sup>38</sup> at 293.15 and 303.15 K; in the dilute region, the values agree with the measurements performed by Romero et al.<sup>39</sup> For 1-butanol, Romero and Páez<sup>40</sup> reported volumetric properties at 298.15 K. The molar volume  $v$  of the mixtures was calculated from the reciprocal of the density (eq 14). Second-degree polynomials were fitted to the plots  $v$  versus  $x_2$ , except for 1-butanol, where a linear fitting was adequate. Partial molar volumes were calculated from eqs 12 and 13.

The number of moles of water and alcohol,  $N_1^b$  and  $N_2^b$ , existing in a bulk of volume  $V$  were determined from eqs 16 and 17. Excess two-dimensional concentrations  $\Gamma_1^{\text{exc}}$  and  $\Gamma_2^{\text{exc}}$  were calculated using eqs 18 and 19. The two-dimensional concentrations in the bulk phase,  $\Gamma_1^{\text{vol}}$  and  $\Gamma_2^{\text{vol}}$ , were

computed according to eq 20, where surface thickness  $d$  was estimated from the partial molar volume of the alcohols, assuming a spherical geometry (eq 23). Addition of concentrations  $\Gamma_i^{\text{exc}}$  and  $\Gamma_i^{\text{vol}}$  provides the absolute surface concentrations  $\Gamma_i$  (eq 21), from which surface molar fractions  $x_i^s$  are obtained (eq 22).

The key point in the procedure described above is the clear differentiation between the concentrations  $\Gamma_2^{(1)}$  and  $\Gamma_2^{\text{exc}}$ , which can be easily misinterpreted as the same quantity. Textbooks describe  $\Gamma_2^{(1)}$  as the excess concentration defined by the Gibbs dividing surface,<sup>8,10</sup> without going deeper into its physical meaning. This is probably why Raina et al. took  $\Gamma_2^{(1)}$  equal to  $\Gamma_2^{\text{exc}}$ , calculating the surface molar fractions of alcohols through eq 33<sup>18,19</sup>

$$x_2^s = \frac{\Gamma_2^{(1)}}{d}(x_1v_1 + x_2v_2) + x_2 \quad (33)$$

where  $d$  is the thickness of the surface, determined in the same way as in this paper. If  $\Gamma_2^{(1)}$  were replaced by  $\Gamma_2^{\text{exc}}$  in eq 33, affording eq 34, it could be said that eqs 34 and 21 are equivalent:

$$\frac{x_2^s}{v}d = \Gamma_2^{\text{exc}} + \frac{x_2d}{v} \quad (34)$$

$v$  is the molar volume ( $x_1v_1 + x_2v_2$ ), strictly given by ( $x_1\bar{v}_1 + x_2\bar{v}_2$ ). The second term on the right-hand side of eq 34 is the bulk two-dimensional concentration  $\Gamma_2^{\text{vol}}$  (eq 20), whereas the term on the left-hand side could be identified as the absolute surface concentration  $\Gamma_2$ . However, the molar volume to be used with  $x_2^s$  should match the surface composition; that is, the molar volume on the left-hand side should be ( $x_1^sv_1 + x_2^sv_2$ ) and not ( $x_1v_1 + x_2v_2$ ), which shows the inaccuracy of eq 33, even if  $\Gamma_2^{(1)}$  were replaced by  $\Gamma_2^{\text{exc}}$ .

In the dilute region, the difference between the bulk and the surface solute concentration is larger than in the concentrated region. Therefore, in the dilute region,  $\Gamma_2^{(1)}$  displays an increasing behavior as shown in Figure 4. A maximum in  $\Gamma_2^{(1)}$  is

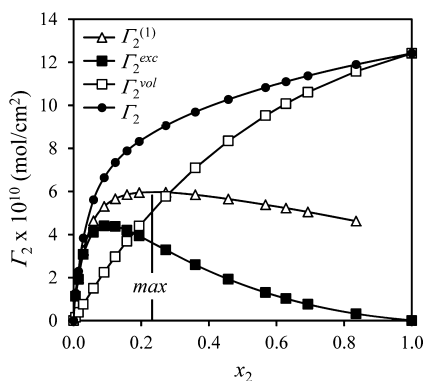


**Figure 4.** Comparison of methanol two-dimensional concentrations  $\Gamma_2^{(1)}$ ,  $\Gamma_2^{\text{exc}}$ ,  $\Gamma_2^{\text{vol}}$ , and  $\Gamma_2$ , at 303.15 K. The lines are a guide for the eye. The vertical line shows the maximum of  $\Gamma_2^{(1)}$ .

attained at the inflection point of the curve  $\pi$  versus  $\ln a_2$  (see eq 10 and Figure 3a, for methanol). This point is ascribed to the proximity to surface saturation conditions. As the solute concentration further increases, approaching 1, the difference between the bulk and the surface compositions diminishes, leading to a decreasing  $\Gamma_2^{(1)}$ , undefined for pure solutes (see eq 7). The excess  $\Gamma_2^{\text{exc}}$  displays a behavior similar to that of  $\Gamma_2^{(1)}$

(see Figure 4), but because the partial molar volumes are considered to be equal in the bulk and in the surface,  $\Gamma_2^{\text{exc}}$  is zero for the pure solutes. Concentrations  $\Gamma_2^{(1)}$  and  $\Gamma_2^{\text{exc}}$  are close to each other only in the high dilute region, where the quotient  $(x_2/x_1) \rightarrow 0$  (see eqs 16 and 18). For the slightly water-soluble 1-butanol, the proximity of  $\Gamma_2^{(1)}$  and  $\Gamma_2^{\text{exc}}$  is shown in Figure 5.

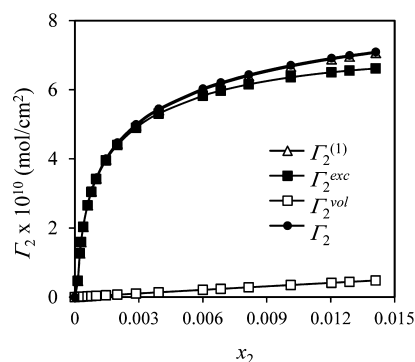


**Figure 5.** Same as Figure 4 but for 1-butanol at 298.15 K, for  $0 < x_2 < 0.0141$ .

Gibbs excess  $\Gamma_2^{(1)}$  has also been misinterpreted as the absolute concentration  $\Gamma_2$  as in the work of Yano,<sup>23</sup> who explains that the maximum of  $\Gamma_2^{(1)}$  is due to the formation of an alcohol monolayer, the reciprocal of which provides an area of  $20 \text{ \AA}^2$  per  $\text{CH}_2$  chain in a close-packed configuration. After the maximum, the following decrement of  $\Gamma_2^{(1)}$  is ascribed to the destruction of the hydrogen bond network of water due to the aggregation of alcohols; in Yano's own words "the surface excess of the alcohols decreases because it is no longer necessary for covering the surface with the solutes when the molecular interactions in the bulk weaken",<sup>23</sup> implying desorption. The maximum of  $\Gamma_2^{(1)}$  due to the formation of a monolayer closely agrees with the proximity to surface saturation conditions, as discussed previously. However, to ascribe the diminishing of  $\Gamma_2^{(1)}$  to alcohols desorption is doubtful. The constant increasing behavior of the absolute concentration  $\Gamma_2$  throughout the whole concentration range, as shown in Figure 4, reflects the continuous adsorption of the alcohols at the surface; otherwise, surface pressure would not be an increasing function of  $x_2$ . According to eq 7,  $\Gamma_2^{(1)}$  and  $\Gamma_2$  approach each other only in the high-dilute interval. As the solute concentration increases, they display different trends: whereas  $\Gamma_2^{(1)}$  decreases,  $\Gamma_2$  increases to the volumetric two-dimensional concentration  $\Gamma_2^{\text{vol}}$  given by eq 20 (see Figure 4).

The calculated surface molar fractions  $x_2^s$  are shown in Figure 6. In all cases,  $x_2^s$  is larger than the bulk molar fraction  $x_2$ , showing alcohol adsorption. Raina et al. determined the composition of the vapor in direct contact with the surface of the aqueous solutions of alcohols.<sup>18,19</sup> The vapor was swept off the surface through a pulsed supersonic valve, and composition was determined by means of TOF-mass spectrometry. For the systems of methanol and 1-butanol, Raina et al.'s data shown in Figures 6a and 7 were read from Figures 5 and 6 of ref 19. For ethanol and 1-propanol, Raina et al. showed that their results were fairly reproduced by the mixing rule of Laaksonen, so only the mixing rule is displayed in panels b and c of Figure 6, plus a few points of the ethanol system taken from ref 18.

For methanol, the surface molar fractions  $x_2^s$  calculated in this work agree with Raina et al.'s data up to a bulk molar

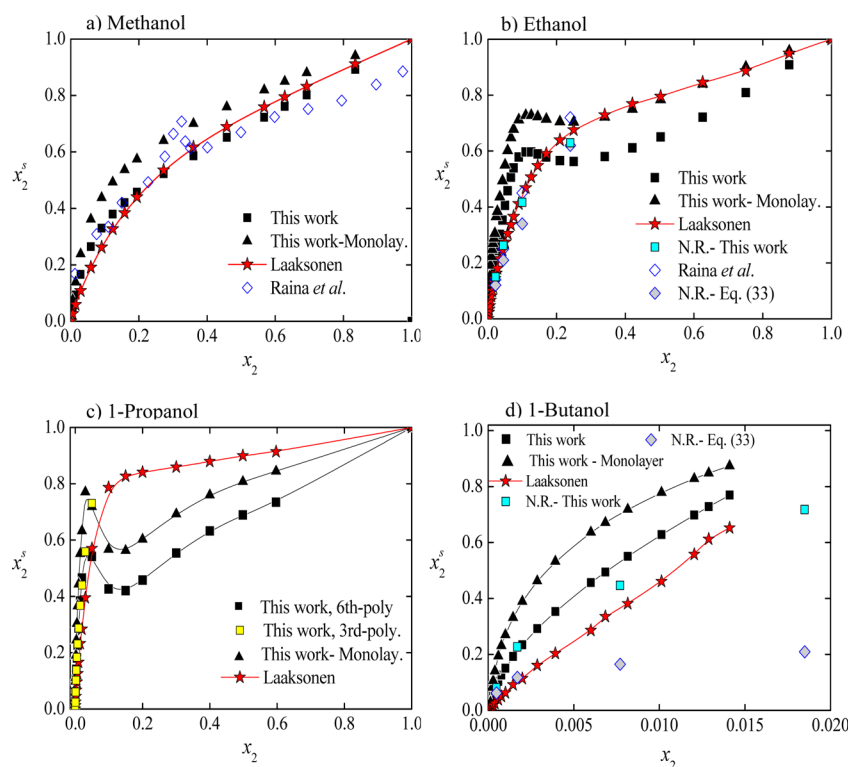


**Figure 6.** Surface molar fraction  $x_2^s$  versus bulk molar fraction  $x_2$  of alcohols. Solid lines are a guide for the eye.

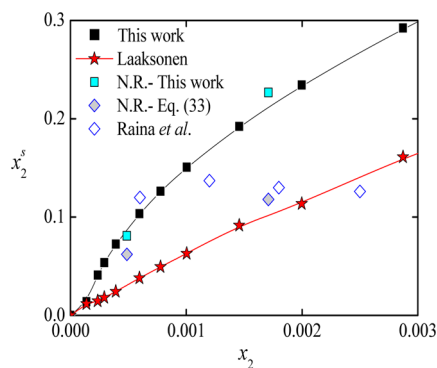


**Figure 7.** Surface molar fraction  $x_2^s$  versus bulk molar fraction  $x_2$  of 1-butanol. Solid lines are a guide for the eye.

fraction  $x_2 = 0.6$ . After this concentration, our results obey the Laaksonen rule, with surface molar fractions approaching 1 as bulk concentration increases. On the contrary, Raina et al.'s data deviate from the Laaksonen rule, with surface molar fractions away from 1, even for the highest concentration shown in Figure 6a. On the basis of the reproducibility of Raina et al.'s data of ethanol and 1-propanol by the Laaksonen rule, it is probable that these deviations are due to experimental errors.

For the aqueous systems of ethanol and 1-propanol, the calculated surface molar fractions do not display a constant increasing behavior in the entire concentration range as in the case of methanol. For ethanol, surface concentration decreases in the interval  $0.11 < x_2 < 0.32$  and for 1-propanol, in the interval  $0.03 < x_2 < 0.15$ . Surface composition is very sensitive to the experimental surface tension data, mainly after the inflection point of the curve  $\pi$  versus  $\ln a_2$ . These results are attributed to the sensitivity of  $\Gamma_2^{(1)}$  to the  $n$ th-degree polynomial fitted to the plot  $\pi$  versus  $\ln a_2$ , as shown below.

This sensitivity becomes more evident after the inflection point (where  $\Gamma_2^{(1)}$  starts decreasing) because at higher concentrations, the change in the concavity makes an accurate fitting more challenging. This problem is not present in the methanol system because surface tension decreases smoothly. Molecular dynamics simulations of aqueous mixtures of methanol show that the methanol surface concentration is an increasing function in the entire concentration interval.<sup>41,42</sup>

For the ethanol system, Li et al.<sup>20</sup> reported  $\Gamma_2^{(1)}$  obtained from neutron reflection (NR) for four different concentrations. Surface composition was calculated from these values by means of eqs 11–22. Table 2 shows that surface molar fractions agree

**Table 2.** Calculated and Experimental Ethanol Surface Molar Fractions  $x_2^s$

$x_2$	NR, this work <sup>a</sup>	Raina et al. <sup>b</sup>	NR, eq 33 <sup>c</sup>
0.022	0.150	0.14	0.12
0.045	0.262	0.25	0.21
0.10	0.417	0.45	0.34
0.24	0.629	0.72	0.62

<sup>a</sup>Calculated from  $\Gamma_2^{(1)}$  reported by Li et al.<sup>20</sup> from neutron reflection (NR) <sup>b</sup>Determined experimentally by Raina et al.<sup>18</sup> <sup>c</sup>Calculated by Raina et al. using eq 33, with  $\Gamma_2^{(1)}$  from ref 20 and with  $d = 5.5 \text{ \AA}$ .<sup>18</sup>

with the experimental data of Raina et al. Actually, Raina et al.'s data are better than they originally thought, but they compared their results with the surface molar fractions provided by eq 33, which has already been demonstrated to be inaccurate. Results of eq 33 are also included in Table 2. The agreement with Raina et al. and with the Laaksonen rule of the surface molar fractions calculated from NR demonstrates that the decreasing behavior shown in Figure 6b is due to the sensitivity of the method to the fitting of an  $n$ th-degree polynomial to the experimental data  $\pi$  versus  $\ln a_2$ , and not due to the theoretical

foundation of the method itself. Results for 1-propanol reinforce this observation. If data after  $x_2 = 0.0497$  are dismissed in Figure 3c and a third-degree polynomial is fitted instead of the sixth-degree polynomial, the resultant surface composition is closer to the Laaaksonen rule, with no maximum, as shown in Figure 6c. The third- and sixth-degree polynomials are barely distinguishable from each other, but the slight change in  $\Gamma_2^{(1)}$  at  $x_2 = 0.0497$ , from 0.040 to 0.046 molecules/Å<sup>2</sup>, originates a change in the surface molar fraction from  $x_2^s = 0.5416$  to  $x_2^s = 0.7306$ . The difficulty of reporting the exact concentration of hygroscopic alcohols and subtle experimental errors in surface tension might contribute as well.

For the aqueous system of 1-butanol, the surface composition determined in this work increases in the entire available interval  $0 < x_2 < 0.141$ . Figure 6d shows that the surface composition calculated from the NR data of Li et al.<sup>21</sup> lies between the surface composition computed from surface tension and the Laaksonen rule. If eq 33 were used, surface molar fractions would be 2–3.5 times smaller. Comparison is shown in Table 3 for the four concentrations reported by Li et

**Table 3. 1-Butanol Surface Molar Fractions  $x_2^s$**

$x_2$	this work <sup>a</sup>	NR, this work <sup>b</sup>	NR, eq 33 <sup>c</sup>
0.0005	0.088	0.081	0.062 <sup>d</sup>
0.0017	0.213	0.227	0.118 <sup>d</sup>
0.0077	0.532	0.447	0.165
0.0185	0.903	0.718	0.209

<sup>a</sup>Calculated from surface tension data. <sup>b</sup>Calculated from  $\Gamma_2^{(1)}$  reported by Li et al.<sup>21</sup> from neutron reflection (NR). <sup>c</sup>Calculated with eq 33, with  $\Gamma_2^{(1)}$  from ref 21 and with  $d = 7$  Å. <sup>d</sup>Read from Figure 6 of ref 19.

al. In the high-dilute region, zoomed in in Figure 7, the procedure developed in this work provides the same results with  $\Gamma_2^{(1)}$  from surface tension or from NR. For this system, calculations do not agree with Raina et al.'s experimental surface molar fractions shown in Figure 7, which are independent of bulk concentration. However, Raina et al. themselves recognize that their method is not accurate enough at dilute concentrations,<sup>19</sup> making their results unreliable.

The thermodynamic consistency of the absolute two-dimensional concentrations  $\Gamma_i$  and the surface molar fractions  $x_i^s$  predicted in this work is demonstrated through the compliance of eq 30. The integral on the right-hand side must reproduce the chemical potential of the solvent, given by eq 31. Numerical integration provides the same results as eq 31 for all of the systems studied in this work (see Figure 8), demonstrating the thermodynamic consistency of eqs 11–22.

**3.2. Surface Composition Obeying Guggenheim's Monolayer Approach.** Surface composition was determined through Guggenheim's monolayer approach, with the solvent concentration  $\Gamma_1$  calculated from the solute concentration  $\Gamma_2$  through eq 25. As shown in Figure 6, surface molar fractions are larger than those predicted with eqs 11–22 because the number of water molecules in a molecularly flat monolayer is smaller than in a surface defined by the alcohols diameters (see Figure 2). Note that all surface molar fractions are <1 due to the use of partial molar areas smaller than the reciprocal of the two-dimensional concentrations.

For ethanol mixtures with  $x_2 \geq 0.34$ , it would seem from Figure 6b that the surface is constituted by a flat monolayer. However, all surface molar fractions determined from Guggenheim's approach lack thermodynamic consistency, as shown in Figure 8: the water chemical potential obtained from eq 30 lies below the chemical potential calculated with eq 31.

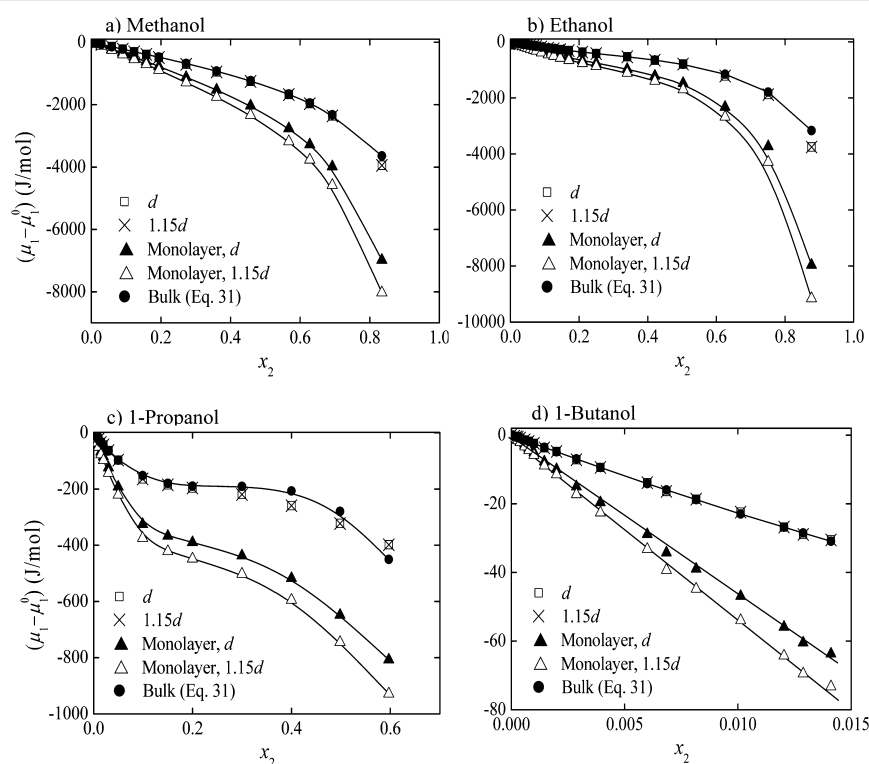


**Figure 8.** Water chemical potential given by eq 30, with absolute surface concentrations following the finite-depth surface layer model and the monolayer model, for surface thicknesses  $d$  and  $1.15d$ .



**3.3. Impact of Surface Thickness on Surface Composition.** Surface molar fractions determined through the procedure developed in this work depend on the thickness of the surface. In all previous calculations, the thickness was estimated from the partial molar volumes of the alcohols, considered as spheres. Thickness was augmented 15% (1.15*d*), representing an average increase of 1 Å, which is of the order of van der Waals radius and covalent bonds.<sup>43</sup> With this augment, surface molar fractions decrease a maximum of 12, 18.5, 25, and 35% for methanol, ethanol, propanol, and 1-butanol systems, respectively. For 1-propanol and 1-butanol, the impact of the thickness on the surface composition is shown in Figure 9.

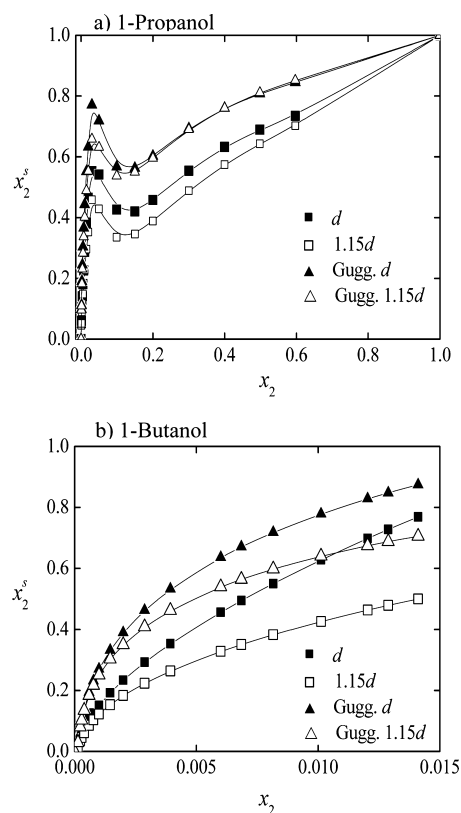


**Figure 9.** Impact of surface thickness on surface molar fractions of 1-propanol and 1-butanol following the finite-depth surface layer model and the monolayer model. For 1-propanol, the sixth-degree polynomial of Figure 3c was used.

Surface molar fractions decrease with increasing thickness because of the incorporation of a larger amount of bulk into the surface ( $\Gamma_i^{\text{vol}}$  is added to  $\Gamma_i^{\text{exc}}$  as shown in Figure 1). Because solute concentration is smaller in the bulk than in the surface, the surface molar fractions become closer to the bulk composition. The impact of the thickness is larger for 1-propanol and 1-butanol due to its higher hydrophobicity in comparison to methanol and ethanol; the more hydrophobic the solute, the larger its adsorption, originating a marked difference between the bulk and the surface concentration.

The thermodynamic consistency test for  $\Gamma_i$  and  $x_i^s$  overcomes the thickness of the surface. The influence of the thickness is canceled in eq 30, reproducing the bulk chemical potential of water given by eq 31, as shown in Figure 8. Therefore, even if surface composition depends on the thickness, the procedure described in section 2.2 is consistent and reliable.

Thickness has less impact on Guggenheim's monolayer model (see Figure 9). Surface molar fractions decrease a maximum of 2, 9, 12, and 19% for methanol, ethanol, 1-propanol, and 1-butanol, respectively. The impact is cushioned by the reduction of the partial molar area, leading to a dampened growth of the product  $a_2\Gamma_2$  in eq 25, making  $\Gamma_1$  not increase as in eq 20. The water chemical potential obtained from eq 30 lies far below the bulk chemical potential (Figure 8), indicating once again the inconsistency of Guggenheim's approach for Gibbs surfaces.

## CONCLUSIONS

General equations for the calculation of the absolute surface concentration of both solute and solvent in a finite-depth surface layer (not a monolayer) were developed, with Gibbs solute excess as the starting point. The procedure relies on the clear understanding of the physical meaning of Gibbs excess in terms of the zero-volume dividing surface and the surface excess defined under the finite-volume surface layer treatment, which may be easily misinterpreted as the same quantity.

Surface molar fractions calculated in this work agree with the experimental results of Raina et al.<sup>18,19</sup> and with the empirical predictions of the Laaksonen mixing rule<sup>16</sup> for the aqueous systems of methanol, ethanol, 1-propanol, and 1-butanol at 298.15 K. Although some surface molar fractions exhibit an odd decreasing behavior within the concentration range where Gibbs excess attains a maximum, it was shown that this trend is due to the sensitivity of the method to the nonlinear fitting of the experimental surface tension data, and not due to the theoretical foundation of the procedure itself. If Gibbs excess is taken from a different source, as from the neutron reflection experiments of Li et al.,<sup>20,21</sup> surface molar fractions are equal to Raina et al.'s results and to the Laaksonen predictions. However, surface tension is a more affordable property than neutron reflection data. The advantage of calculating the absolute surface composition obeying theoretical concepts and not following Laaksonen rule is that the absolute surface composition is ascribed to a specific finite-volume layer, even if the concentration is reported as a two-dimensional quantity; the Laaksonen rule does not provide this information. Now, composition-dependent thermodynamic properties can be assessed.

The general equations developed in this work proved to be consistent with Gibbs–Duhem equations despite the fact that surface composition depends on the surface thickness. The same cannot be said for Guggenheim's monolayer approach, which, in addition, does not reproduce the surface composition of the studied systems, casting doubt on Yano's conclusion about the formation of an alcohol monolayer.<sup>23</sup> Yano's reasoning seems to be founded on the misinterpretation of Gibbs excess and the absolute surface composition, concepts that are clarified in this paper and which do not support a monolayer model for the surface of water-soluble alcohols.

## AUTHOR INFORMATION

### Corresponding Author

\*(J.G.-F.) Mail: Departamento de Fisicoquímica, Facultad de Química, Universidad Nacional Autónoma de México, Ciudad Universitaria, Ave. Universidad 3000, México D.F. 04510, Mexico. Phone: + 52 55 56223899, ext. 44462. Fax: + 52 55 56162010. E-mail: jgraciaf@unam.mx.

## Notes

The authors declare no competing financial interest.

## ACKNOWLEDGMENTS

This work was supported by Dirección General de Asuntos del Personal Académico (DGAPA-UNAM) under Project PAPIIT-IN114015. C.B.-S. thanks Consejo Nacional de Ciencia y Tecnología (CONACyT) for Grant 223384.

## REFERENCES

- (1) Phan, C. M.; Nguyen, C. V.; Yusa, S.-i.; Yamada, N. L. Synergistic adsorption of MIBC/CTAB at the air/water interface and applicability of Gibbs adsorption equation. *Langmuir* **2014**, *30*, 5790–5796.
- (2) Yunfei, H.; Yazhuo, S.; Honglai, L.; Dominique, L.; Anniina, S. Surfactant adsorption onto interfaces: measuring the surface excess in time. *Langmuir* **2012**, *28*, 3146–3151.
- (3) Bermúdez-Salguero, C.; Gracia-Fadrique, J. Activity coefficients from Gibbs adsorption equation. *Fluid Phase Equilib.* **2012**, *330*, 17–23.
- (4) Luo, G.; Bu, W.; Mihaylov, M.; Kuzmenko, I.; Schlossmann, M. L.; Soderholm, L. X-ray reflectivity reveals a nonmonotonic ion-density profile perpendicular to the surface of  $\text{ErCl}_3$  aqueous solutions. *J. Phys. Chem. C* **2013**, *117*, 19082–19090.
- (5) Strey, R.; Viisen, Y.; Aratono, M.; Kratochvil, J. P.; Yin, Q.; Friberg, S. E. On the necessity of using activities in the Gibbs equation. *J. Phys. Chem. B* **1999**, *103*, 9112–9116.
- (6) Radke, C. J. Gibbs adsorption equation for planar fluid-fluid interfaces: invariant formalism. *Adv. Colloid Interface Sci.* **2014**, DOI: 10.1016/j.cis.2014.01.001.
- (7) Aveyard, R.; Haydon, D. A. *An Introduction to the Principle of Surface Chemistry*; Cambridge University Press: Cambridge, UK, 1973.
- (8) Hiemenz, P. C.; Rajagopalan, R. *Principles of Colloid and Surface Chemistry*, 3rd ed.; Dekker: New York, 1997.
- (9) Joos, P. *Dynamic Surface Phenomena*; VSP BV: Zeist, The Netherlands, 1999.
- (10) Rosen, M. J.; Kunjappu, J. T. *Surfactant and Interfacial Phenomena*, 4th ed.; Wiley: Hoboken, NJ, USA, 2012.
- (11) Ross, R.; Chen, E. S. Adsorption and thermodynamics at the liquid-liquid interface. *Ind. Eng. Chem.* **1965**, *57*, 40–52.
- (12) Guggenheim, E. A.; Adam, N. K. The thermodynamics of adsorption at the surface of solutions. *Proc. R. Soc. London, A* **1933**, *139*, 218–236.
- (13) Piñeiro, A.; Brocos, P.; Amigo, A.; Gracia-Fadrique, J.; Lemus, M. G. Extended Langmuir isotherm for binary liquid mixtures. *Langmuir* **2001**, *17*, 4261–4266.
- (14) Salonen, M.; Malila, J.; Napari, I.; Laaksonen, A. Evaluation of surface composition of surface active water–alcohol type mixtures: a comparison of semiempirical models. *J. Phys. Chem. B* **2005**, *109*, 3472–3479.
- (15) Eberhart, J. G. The surface tension of binary liquid mixtures. *J. Phys. Chem.* **1966**, *70*, 1183–1186.
- (16) Laaksonen, A. Nucleation of binary water–*n*-alcohol vapors. *J. Chem. Phys.* **1992**, *97*, 1983–1989.
- (17) Connors, K. A.; Wright, J. L. Dependence of surface tension on composition of binary aqueous-organic solutions. *Anal. Chem.* **1989**, *61*, 194–198.
- (18) Raina, G.; Kulkarni, G. U.; Rao, C. N. R. Mass spectrometric determination of the surface composition of ethanol-water mixtures. *Int. J. Mass Spectrom.* **2001**, *212*, 267–271.
- (19) Raina, G.; Kulkarni, G. U.; Rao, C. N. R. Surface enrichment in alcohol-water mixtures. *J. Phys. Chem. A* **2001**, *105*, 10204–10207.
- (20) Li, Z. X.; Lu, J. R.; Styrkas, D. A.; Thomas, R. K.; Rennie, A. R.; Penfold, J. The structure of the surface of ethanol-water mixtures. *Mol. Phys.* **1993**, *80*, 925–939.
- (21) Li, Z. X.; Lu, J. R.; Thomas, R. K.; Rennie, A. R.; Penfold, J. Neutron reflection study of butanol and hexanol adsorbed at the surface of their aqueous solutions. *J. Chem. Soc., Faraday Trans.* **1996**, *92*, 565–572.
- (22) Li, P. X.; Li, Z. X.; Shen, H.-H.; Thomas, R. K.; Penfold, J.; Lu, J. R. Application of the Gibbs equation to the adsorption of nonionic surfactants and polymers at the air-water interface: comparison with surface excesses determined directly using neutron reflectivity. *Langmuir* **2013**, *29*, 9324–9334.
- (23) Yano, Y. F. Correlation between surface and bulk structures al alcohol-water mixtures. *J. Colloid Interface Sci.* **2005**, *284*, 255–259.
- (24) Bermúdez-Salguero, C.; Gracia-Fadrique, J. Surface chemical potential from a surface equation of state vs. Butler's equation. *Fluid Phase Equilib.* **2014**, *375*, 367–372.
- (25) Prausnitz, J. M.; Lichtenthaler, R. M.; Gomes de Azevedo, E. *Termodinámica Molecular de los Equilibrios de Fases*, 3rd ed.; Prentice Hall: Madrid, Spain, 2000.
- (26) Smith, J. M.; van Ness, H. C.; Abbott, M. M. *Introducción a la Termodinámica en Ingeniería Química*, 6th ed.; McGraw Hill: Mexico, 2001.
- (27) Douillard, J. M. Experimental approach of the relation between surface tension and interfacial thickness of simple liquids. *J. Colloid Interface Sci.* **2009**, *337*, 307–310.
- (28) Sprow, F. B.; Prausnitz, J. M. Surface tensions of simple liquid mixtures. *Trans. Faraday Soc.* **1966**, *62*, 1105–1111.
- (29) Santos, M. S. C. S.; Reis, J. C. R. New thermodynamics for evaluating the surface-phase enrichment in the lower surface tension component. *ChemPhysChem* **2014**, *15*, 2834–2843.
- (30) Ghasemian, E. Prediction of surface tension and surface properties of organic binary mixtures. *J. Mol. Liq.* **2013**, *183*, 64–71.
- (31) Vázquez, G.; Álvarez, E.; Navaza, J. M. Surface tension of alcohol + water from 20 to 50 °C. *J. Chem. Eng. Data* **1995**, *40*, 611–614.
- (32) Livingston, J.; Morgan, R.; Neidle, M. The weight of a falling drop and the laws of Tate, XVIII. The drop weights, surface tensions and capillary constants of aqueous solutions of ethyl, methyl and amyl alcohols, and of acetic and formic acid. *J. Am. Chem. Soc.* **1913**, *35*, 1856–1865.
- (33) Habrdová, K.; Hovorka, S.; Bartovska, L. Concentration dependence of surface tension for very dilute aqueous solutions of organic nonelectrolytes. *J. Chem. Eng. Data* **2004**, *49*, 1003–1007.
- (34) Gmehling, J.; Onken, U.; Rarey-Nies, J. R. *Vapor-Liquid Equilibrium Data Collection. Aqueous Systems*, Suppl. 2 (in Chemistry Data Series Vol. 1, part 1b); DECHEMA: Frankfurt, Germany, 1988.
- (35) Kojima, K.; Zhang, S.; Hiaki, T. Measuring methods of infinite dilution activity coefficients and a database for systems including water. *Fluid Phase Equilib.* **1997**, *131*, 145–179.
- (36) González, B.; Calvar, N.; Gómez, E.; Domínguez, A. Density, dynamic viscosity, and derived properties of binary mixtures of methanol or ethanol with water, ethyl acetate, and methyl acetate at  $T = (293.15, 298.15 \text{ and } 303.15) \text{ K}$ . *J. Chem. Thermodyn.* **2007**, *39*, 1578–1588.
- (37) Zarei, H. A.; Jalili, F.; Assadi, S. Temperature dependence of the volumetric properties of binary and ternary mixtures of water (1) + methanol (2) + ethanol (3) at ambient pressure (81.5 kPa). *J. Chem. Eng. Data* **2007**, *52*, 2517–2526.
- (38) Zarei, H. A.; Shahvarpour, S. Volumetric properties of binary and tertiary liquid mixtures of 1-propanol (1) + 2-propanol (2) + water (3) at different temperatures and ambient pressure (81.5 kPa). *J. Chem. Eng. Data* **2008**, *53*, 1660–1668.
- (39) Romero, C. M.; Páez, M. S.; Pérez, D. A comparative study of the volumetric properties of dilute aqueous solutions of 1-propanol, 1,2-propanediol, 1,3-propanediol, and 1,2,3-propanetriol at various temperatures. *J. Chem. Thermodyn.* **2008**, *40*, 1645–1653.
- (40) Romero, C. M.; Páez, M. S. Volumetric properties of aqueous binary mixtures of 1-butanol, butanediols, 1,2,4-butanetriol and butanetetrol at 298.15 K. *J. Solution Chem.* **2007**, *36*, 237–245.
- (41) Pártay, L. B.; Jedlovsky, P.; Vincze, Á.; Horvai, G. Properties of free surface of water-methanol mixtures. Analysis of the truly interfacial molecular layer in computer simulation. *J. Phys. Chem. B* **2008**, *112*, 5428–5438.

- (42) Darvas, M.; Pártay, L. B.; Jedlovsky, P.; Horvai, G. Computer simulation and ITIM analysis of the surface of water-methanol mixtures containing traces of water. *J. Mol. Liq.* **2010**, *153*, 88–93.
- (43) Morrison, R. T.; Boyd, R. N. *Química Orgánica*, 3rd ed.; Fondo Educativo Interamericano: Boston, MA, USA, 1976.